Saudi Pharmaceutical Journal (2016) **24**, 92–103

King Saud University

Saudi Pharmaceutical Journal

www.ksu.edu.sa
www.sciencedirect.com

ORIGINAL ARTICLE

An integrated Taguchi and response surface methodological approach for the optimization of an HPLC method to determine glimepiride in a supersaturatable self-nanoemulsifying formulation

Rajendra Narayan Dash [a], **Habibuddin Mohammed** [b,*], **Touseef Humaira** [b]

[a] *Alliance Institute of Advanced Pharmaceutical & Health Sciences, Plot No. 64, Survey No. 145, Sardar Patel Nagar, Kukatpally, Hyderabad 500 072, Telangana, India*
[b] *Adept Pharma and Bioscience Excellence Private Limited, Corporate Office: 10-3-561/3/A/102, Vijayanagar Colony, Hyderabad 500057, Telangana, India*

Received 11 February 2015; accepted 11 March 2015
Available online 23 March 2015

KEYWORDS

Taguchi orthogonal array;
Signal-to-noise ratio;
Response surface methodology;
S-SNEDDS;
Optimization;
HPLC method

Abstract We studied the application of Taguchi orthogonal array (TOA) design during the development of an isocratic stability indicating HPLC method for glimepiride as per TOA design; twenty-seven experiments were conducted by varying six chromatographic factors. Percentage of organic phase was the most significant ($p < 0.001$) on retention time, while buffer pH had the most significant ($p < 0.001$) effect on tailing factor and theoretical plates. TOA design has shortcoming, which identifies the only linear effect, while ignoring the quadratic and interaction effects. Hence, a response surface model for each response was created including the linear, quadratic and interaction terms. The developed models for each response found to be well predictive bearing an acceptable adjusted correlation coefficient (0.9152 for retention time, 0.8985 for tailing factor and 0.8679 for theoretical plates). The models were found to be significant ($p < 0.001$) having a high F value for each response (15.76 for retention time, 13.12 for tailing factor and 9.99 for theoretical plates). The optimal chromatographic condition uses acetonitrile – potassium dihydrogen phosphate (pH 4.0; 30 mM) (50:50, v/v) as the mobile phase. The temperature, flow rate and injection volume were

Abbreviations: GLP, Glimepiride; S-SNEDDS, Supersaturatable self-nanoemulsifying drug delivery system; TOA, Taguchi orthogonal array; S/N, signal-to-noise; RSM, response surface methodology; d_G, global desirability

* Corresponding author. Tel./fax: +91 4066103388.
E-mail address: drhabib21@gmail.com (H. Mohammed).

Peer review under responsibility of King Saud University.

Production and hosting by Elsevier

http://dx.doi.org/10.1016/j.jsps.2015.03.004

selected as 35 ± 2 °C, 1.0 mL min^{-1} and 20 μL respectively. The method was validated as per ICH guidelines and was found to be specific for analyzing glimepiride from a novel supersaturatable self-nanoemulsifying formulation.

1. Introduction

Glimepiride (GLP): {N-[4-[2-(3-ethyl-4-methyl-2-oxo-3-pyrroline-1-carboxamido)-ethyl]-benzenesulfonyl]-N′-4-methylcyclohexylurea} is a sulfonylurea antidiabetic drug. It is given orally for the treatment of type II diabetes mellitus and lower blood glucose by stimulating the insulin release from pancreatic β cell (Sweetman, 2009). GLP is a poorly water-soluble drug having a logP (octanol/water) value of 3.81 with a pKa of 6.2 (Brittain, 2009).

Self-nanoemulsifying drug-delivery systems are technological advances of lipid based drug delivery with a huge potential to improve oral bioavailability of poorly soluble drug (Bandyopadhyay et al., 2012). More recently, there has been an increasing focus on the application of the supersaturatable self-nanoemulsifying drug delivery system (S-SNEDDS) (Gao and Morozowich, 2006; Wei et al., 2012). S-SNEDDS preconcentrates are an isotropic mixture of oil, surfactant, co-surfactant, polymeric precipitation inhibitor (PPI) and drug that forms a fine oil-in-water nanoemulsion, when introduced into an aqueous medium under mild agitation. The PPI prevents the drug from precipitating out of the solution, thus maintaining a supersaturated state (Gao et al., 2009). With this direction, S-SNEDDS for GLP was formulated to enhance its solubility (unpublished data).

However, there was a need to develop a robust stability indicating method to quantify GLP during drug excipients compatibility testing as well as for routine assay and stability studies of the said formulation. Numbers of HPLC methods exist to quantify GLP alone or in combination from pharmaceutical dosage form (Bansal et al., 2008; Bonfilio et al., 2013; El-Enany et al., 2012; El Deeb et al., 2006; Jain et al., 2008; Karthik et al., 2008; Khan et al., 2005; Kovaríková et al., 2004; Lakshmi and Rajesh, 2011; Maier et al., 2009; Pandit et al., 2012; Shaodong et al., 2010; Yao et al., 2007) and biological matrices (Aburuz et al., 2005; Chakradhar et al., 2008; El-Enany et al., 2012; Lakshmi and Rajesh, 2011; Musmade et al., 2011; Pistos et al., 2005; Polagani et al., 2013; Salem et al., 2004; Samala, 2011; Tripathi et al., 2013). However, neither of the methods discuss regarding quantitative estimation of GLP from emulsions as the final product. Operating parameters such as the percentage of organic phase, mobile phase pH, flow rate, injection volume, buffer molarity, and temperature play a critical role in controlling selectivity in reverse phase HPLC separations (Ahuja and Rasmussen, 2007). Hence, Proper optimization of the chromatographic parameters is needed to achieve a chromatogram having a desired system suitability parameter. The conventional way of optimizing an HPLC method that uses the one-factor-at-a-time (OFAT) approach has its own limitations as this approach is time-consuming, requires a larger number of experiments, and frequently fails to project the true optimal condition (Bezerra et al., 2008). In most situations, the developed method requires further improvement thus slowing the drug development process (Awotwe-Otoo et al., 2012).

An experimental design approach by which multivariate data can be handled and fitted to an empirical function offers a better choice over OFAT for identification and control of critical factors (Hibbert, 2012). TOA design, which offers recognition of the factor's main effect in relatively few experiments, is being used widely in the manufacturing section for its robust optimization of process parameters (Aggarwal et al., 2008; Chang et al., 2007; Kwak, 2005). Taguchi orthogonal array (TOA) design uses a special set of arrays, gives the minimum number of experiments with maximum information about the influence of factors involved in the study. The term "orthogonal" means balanced, separable or not mixed; hence, the influence of an individual factor is not mixed up with the influence of other factors and is separated as a main effect of the said factor (Taguchi, 1987). The effect of a single factor can be a linear, quadratic or higher order, but the model assumes that there are no interactions among the individual factors (Montgomery, 2013). Hence, to overcome these shortcomings of TOA design, as an additional measure, a response surface methodology (RSM) was applied to create a mathematical model for each response that can be used to predict the optimal condition. A combined TOA design and RSM approach, which offers an edge over TOA design alone, has been widely used for process optimization (Kwak, 2005; Sarıkaya and Güllü, 2014).

The aim of our study was to apply a TOA design combined with RSM for robust optimization of a stability indicating HPLC method for GLP with enhanced system suitability parameters that can be used for subsequent assay of GLP from an S-SNEDDS formulation.

2. Materials and methods

2.1. Chemicals and reagents

GLP USP was kindly supplied by Alembic Ltd. (Vadodara, India). EP/NF grade medium chain tri-glycerides (Captex® 300) and medium chain mono-glycerides (Capmul® MCM) were supplied by Abitec Corp., Janesville, USA. EP grade poly-glycol mono and di-esters of 12-hydroxy stearic acid (Solutol® HS 15) was provided by BASF SE, Ludwigshafen, Germany. Hydroxypropyl methylcellulose grade E5 (HPMC E5) was supplied by Colorcon Asia Pvt. Ltd., Mumbai, India. Size "1" hard gelatin capsule shell was supplied by Capsugel Health Care Ltd., Mumbai, India. Methanol (HPLC), acetonitrile (HPLC), potassium dihydrogen phosphate (chromatography), sodium metabisulphite (AR), calcium carbonate (GR) and talc (GR) were purchased from Merck Specialties Pvt. Ltd., Mumbai, India. Ortho phosphoric acid (AR), hydrochloric acid (37% v/v) (AR), sodium hydroxide (AR) and hydrogen peroxide (30% v/v) (AR) were

purchased from SD Fine-Chem. Ltd., Mumbai, India. 18 MΩ Water (HPLC grade) was obtained in-house from a Direct Q-3 UV water purification system (Millipore India Pvt. Ltd., Bengaluru, India).

2.2. Equipment

The HPLC system consisted of a quaternary pump (series 200, Perkin Elmer), auto sampler (series 200, Perkin Elmer), and temperature-controlled column oven (series 200, Perkin Elmer). The UV–VIS detector (series 200, Perkin Elmer) was operated at a wavelength of 229 nm. Data collection and analyses were performed using Totalchrom workstation, version 6.3.1.0504 (Perkin Elmer Inc., USA). Columns used were Luna C8, 100 × 4.6 mm, 3.0 μm (Phenomenex, USA), and Hypersil BDS C8, 100 × 4.6 mm, 3 μm (Thermo Scientific, UK).

2.3. Preparation of stock and standard solution

The stock solution of GLP (1000 μg mL^{-1}) was prepared in methanol. The standard solution (100 μg mL^{-1}) was prepared by diluting the stock solution in methanol. The calibration samples were prepared by dilution of the standard solution with the mobile phase. The buffer was prepared by dissolving 4082 mg (30 mM) of potassium dihydrogen phosphate in 1 L of HPLC grade water, and the pH was adjusted to 4.0 with *o*-phosphoric acid.

2.4. Design of experiment

A six-factor three-level TOA design consisted of L_{27} array (3^6) for the optimization of the HPLC method. The factors selected were percentages (v/v) of acetonitrile (A), buffer pH (B), flow rate (mL min^{-1}) (C), injection volume (μL) (D), column oven temperature (°C) (E) and buffer molarity (mM) (F). The experimental plans were designed using Minitab® version 16 (Minitab, Inc. Coventry, UK). The scheme of experimental design is presented in Table 1. As per the TOA design, twenty-seven experiments were performed to evaluate the responses such as retention time (RT), tailing factor (TF), and theoretical plates (TP). The goal of this optimization was set to minimize the tailing factor (⩽2.0) and maximize theoretical plates (>2500) on a minimum run time with an acceptable resolution (⩾1.8) between GLP and its nearest degradation peak. However, the resolution between GLP and degradants was not considered as a response due to the discontinuities of the resolution with changes in selectivity (Rafamantanana et al., 2012).

Signal-to-noise (S/N) ratio, which is an important quality characteristics of TOA design, was computed as below in Eq. (1).

$$S/N = -10\left[\frac{1}{n}(y_1^2 + y_2^2 + \ldots + y_n^2)\right] \quad (1)$$

where y_1, y_2, …, y_n are the responses for a trial condition repeated n times and S/N ratio of each response was computed for each trial. The main effects of factors along with their percentage contribution were computed. The difference between highest and lowest values of S/N ratio or means was used to calculate the delta values. The delta values along with percentage contributions were used to rank the individual factor (Shaligram et al., 2008). Main effect analysis of variance (main effect ANOVA) was applied to validate the developed model. Statistical "p value" less than 0.05 ($p < 0.05$) was considered as significant.

Similarly, for RSM models, the experimental data were analyzed by response surface regression using Statistica® version 10.0 (Stat soft, Inc., Tulsa, OK, USA). A second order polynomial equation satisfying the linear, quadratic and interaction effects of six studied factors was generated as below in Eq. (2).

$$\begin{aligned} Y = {} & \beta_0 + \beta_1 X_1 + \beta_{11} X_1^2 + \beta_2 X_2 + \beta_{22} X_2^2 + \beta_3 X_3 + \beta_{33} X_3^2 \\ & + \beta_4 X_4 + \beta_{44} X_4^2 + \beta_5 X_5 + \beta_{55} X_5^2 + \beta_6 X_6 \\ & + \beta_{66} X_6^2 \beta_{12} X_1 X_2 + \beta_{13} X_1 X_3 + \beta_{23} X_2 X_3 + \beta_{14} X_1 X_4 \\ & + \beta_{24} X_2 X_4 + \beta_{34} X_3 X_4 + \beta_{16} X_1 X_6 + \beta_{26} X_2 X_6 \\ & + \beta_{36} X_3 X_6 + \beta_{46} X_4 X_6 + \beta_{15} X_1 X_5 + \beta_{25} X_2 X_5 \\ & + \beta_{35} X_3 X_5 + \beta_{45} X_4 X_5 + \beta_{65} X_6 X_5 \end{aligned} \quad (2)$$

where Y, the response to be modeled; β_0, the arithmetic mean response; β_1, β_2, β_3, β_4, β_5 and β_6 are the regression coefficient of factors X_1, X_2, X_3, X_4, X_5 and X_6 respectively.

A positive coefficient indicates a synergistic effect, while a negative one represents an antagonistic effect of the concerned factor upon the response Y.

Contour graphs were drawn to visualize the region of optimum chromatographic conditions. Residual plots were constructed and inspected to test the adequacies of the developed models. Analysis of variance (ANOVA) was applied to validate the developed models. Derringer's desirability was computed and was used along with S/N ratio and other statistical parameters to optimize the method satisfying optimization goal.

2.5. Method validation

To confirm its suitability for its intended purpose, the method was validated in accordance with the ICH guidelines (ICH Q2R1, 2005) for system suitability, linearity, specificity, precision, accuracy, limit of detection, limit of quantification and robustness.

2.5.1. Linearity

Linearity was evaluated by injecting a series of ranging from 0.05 to 200 μg mL^{-1}, including 0.05, 0.1, 0.2, 0.5, 1, 5, 10, 20, 30, 50, 70, 100, 150, and 200 μg mL^{-1}. 20 μL injections were made six times for above concentrations. A linear regression analysis was performed between the employed concentrations (μg mL^{-1}) and peak areas (μV s) obtained.

2.5.2. Precision

The precisions of the proposed HPLC method were determined by injecting three different concentrations at low (LOQ), mid and high end of the calibration curve. The selected concentrations were 0.05, 30, and 100 μg mL^{-1}. For intra-day variation, sets of six replicates of the above three concentrations were analyzed on the same day; for inter-day variation, six replicates were analyzed on six different days.

Table 1 Scheme of experimental design for HPLC method development of GLP.

Run	A	B	C	D	E	F	Retention time (min)		Tailing factor		Theoretical plates	
							Observed	Predicted	Observed	Predicted	Observed	Predicted
1	30	3.00	0.50	10	25.0	10	25.17	24.12	0.99	0.98	4156	4143
2	30	3.00	0.50	10	32.5	25	13.51	13.97	1.06	1.04	6522	6378
3	30	3.00	0.50	10	40.0	40	10.74	11.32	1.13	1.14	8341	8496
4	30	4.75	0.85	20	25.0	10	18.88	21.02	1.11	1.11	6895	7116
5	30	4.75	0.85	20	32.5	25	11.72	10.69	1.12	1.13	8112	8005
6	30	4.75	0.85	20	40.0	40	8.99	7.87	1.22	1.19	8892	8776
7	30	6.50	1.20	30	25.0	10	25.50	24.40	1.41	1.40	9712	9502
8	30	6.50	1.20	30	32.5	25	13.32	13.88	1.41	1.40	8794	9044
9	30	6.50	1.20	30	40.0	40	10.35	10.88	1.42	1.42	8510	8469
10	45	3.00	0.85	30	25.0	25	6.04	5.34	1.27	1.21	6627	6309
11	45	3.00	0.85	30	32.5	40	4.77	5.19	1.30	1.33	6502	6364
12	45	3.00	0.85	30	40.0	10	9.06	9.33	1.06	1.07	5091	5545
13	45	4.75	1.20	10	25.0	25	5.49	5.16	1.21	1.25	7315	7122
14	45	4.75	1.20	10	32.5	40	4.65	3.59	1.31	1.27	7310	7223
15	45	4.75	1.20	10	40.0	10	7.75	9.13	1.13	1.12	7485	7764
16	45	6.50	0.50	20	25.0	25	15.72	16.74	1.43	1.44	9015	9524
17	45	6.50	0.50	20	32.5	40	12.52	13.15	1.48	1.47	8575	8799
18	45	6.50	0.50	20	40.0	10	26.73	25.07	1.41	1.40	13021	12286
19	60	3.00	1.20	20	25.0	40	2.67	4.32	1.50	1.50	5674	6408
20	60	3.00	1.20	20	32.5	10	4.75	4.11	1.16	1.16	6273	6048
21	60	3.00	1.20	20	40.0	25	3.13	2.10	1.32	1.30	6819	6309
22	60	4.75	0.50	30	25.0	40	6.24	4.85	1.50	1.50	6161	5881
23	60	4.75	0.50	30	32.5	10	9.98	11.03	1.22	1.25	8382	8468
24	60	4.75	0.50	30	40.0	25	6.67	6.99	1.44	1.39	7712	7904
25	60	6.50	0.85	10	25.0	40	6.96	6.68	1.47	1.45	6079	5624
26	60	6.50	0.85	10	32.5	10	14.68	14.25	1.34	1.30	9432	9569
27	60	6.50	0.85	10	40.0	25	8.10	8.79	1.30	1.35	8735	9052

A, percentage (v/v) of acetonitrile; B, buffer pH; C, flow rate (mL min^{-1}); D, injection volume (μL); E, temperature of column oven (°C) and F, buffer molarity (mM).

2.5.3. Accuracy

Accuracy of the developed method was tested by fortifying a mixture of degraded samples with the three different concentrations of GLP (16, 20, and 24 μg mL^{-1} equivalent to 1.6, 2.0, and 2.4 mg) at 80%, 100%, and 120% levels and determining the recovery of added drug. The peak area of the standard was calculated by taking the difference between the peak area of fortified and unfortified samples. Three replicates of each concentration level were prepared and injected. The percentage recoveries of GLP at each level ($n = 3$), along with mean percentage recovery from total injections ($n = 9$) were determined.

2.5.4. LOD and LOQ

Limit of detection (LOD) was defined as the lowest concentration of GLP resulting in a signal-to-noise ratio of 3:1, and limit of quantification (LOQ) was expressed as a signal-to-noise ratio of 10:1. Due to the difference in detector response, varied concentrations ranging between 0.01 and 0.1 μg mL^{-1} were prepared and analyzed.

2.5.5. Specificity

Specificity is the ability to assess unequivocally the analyte in the presence of components, which may be expected to be present. Typically, these might include impurities, degradants, matrix, etc. The specificity of the assay was determined by the complete separation of GLP in the presence of its degradation products generated under stress conditions as well as from the excipients of GLP S-SNEDDS.

2.5.6. Robustness of the method

Robustness of any analytical procedure is "a measure of its capacity to remain unaffected by small, but deliberate variations in method parameters and provides an indication of its suitability during normal usage" (International conference on harmonisation of technical requirements for registration of pharmaceuticals for human use, 2005). A method is robust if it is unaffected by small changes in operating conditions. Robustness of the method was evaluated by deliberately altering few parameters. The parameters included variation of C-8 columns from different manufacturers, the percentage (v/v) of acetonitrile in the mobile phase, buffer pH, flow rate (mL min^{-1}), column oven temperature (°C) and buffer molarity (mM). Two analytical columns, one Luna C8, 100 × 4.6 mm, 3.0 μm (Phenomenex, USA), and the other Hypersil BDS C8, 100 × 4.6 mm, 3 μm (Thermo Scientific, UK) were used during the experiment. Composition of acetonitrile in mobile phase was varied by 50 ± 1.0 percentages (v/v), while buffer pH was varied by 4.0 ± 0.1 units. The flow rate was varied by 1.0 ± 0.05 mL min^{-1}, column oven temperature was varied by 35 ± 2 °C, and buffer molarity was varied by 30 ± 2 mM. Each factor selected (except columns from different manufacturers), were changed at three levels. One factor at a time was changed to estimate the effect. Replicate injections ($n = 6$) of standard solution (20 μg mL^{-1}) were performed under small changes of above six chromatographic parameters. The mean ± SD ($n = 6$) of response was calculated for each level variation due to a particular factor. In addition, the

mean ± SD along with% RSD was calculated for all three or two levels ($n = 18$ or $n = 12$) for each factor.

2.5.7. System suitability

System-suitability test for retention time, theoretical plates and tailing factor, was evaluated for six replicates injections of GLP (20 μg mL^{-1}).

2.6. Forced degradation studies

The stability indicating the nature of the developed HPLC method was studied by forced degradation of GLP under following stressed conditions. The resultant solutions from different conditions were diluted with mobile phase to obtain GLP concentration equal to 20 μg mL^{-1}.

2.6.1. Hydrolytic conditions: acid, alkali, and water induced degradation

Two mL of the standard stock solution was transferred to each of three 10-mL volumetric flasks, and the volume was made up to the mark with 2 M hydrochloric acid, 1 M sodium hydroxide, and water separately. Acid and base induced degradation samples were kept at room temperature for 48 h while the hydrolytic induced degradation sample was kept for 5 days at 80 °C in a thermostatic oven.

2.6.2. Oxidizing conditions: hydrogen peroxide induced degradation

Two mL of the standard stock solution was transferred to a 10-mL volumetric flask, and the volume was made up to the mark with 3% (v/v) H_2O_2. This was kept at room temperature for 6 h.

2.6.3. Thermal conditions: dry heat and moist heat induced degradation

Two mL of the standard stock solution was transferred to each of two 10-mL volumetric flask, and the volume was made up to the mark with methanol. These were kept at 80 °C in a thermostatic oven and water bath respectively. Dry heat and moist heat samples were stressed for 24 h and 48 h respectively.

2.6.4. Photochemical degradation

Two mL of the standard stock solution was transferred into a 10-mL volumetric flask and made the volume up to the mark with methanol and was kept under direct sunlight for seven days.

2.7. Sample collection, storage, and preparation

Before collecting samples, volume was made up to the mark with respective solvent. One mL of the sample was collected from each stressed condition. The samples from acid, base and oxidation induced degradation were neutralized by adding 1 mL of appropriate strength of sodium hydroxide, hydrochloric acid, and sodium metabisulphite. All samples were stored at 2–8 °C in the refrigerator before analysis. On the day of analysis, samples were diluted with mobile phase up to 10 mL and mixed.

A degradation mixture was prepared by mixing 1 mL of diluted samples from all conditions. Prior to injection into HPLC, all samples were filtered with 0.22 μm membrane syringe filter. At first, the degradation mixture was injected to optimize the run time, followed by injection of the individual degradation samples six times.

2.8. Preparation of GLP S-SNEDDS and determination of drug content

The S-SNEDDS of GLP was prepared by dissolving GLP (0.25 g) into a 10 g mixture of Oil/Captex® 300 (30% w/w), Surfactant/Solutol® HS 15 (45% w/w) and Co-surfactant/Capmul® MCM (25% w/w). The mixtures were mixed for 5 min with a Cyclo-mixer (Remi, model CM101, Mumbai, India) to get a clear solution. 5% w/w equivalent to 0.5 g of HPMC E5 (PPI) was added to the above solution and was mixed vigorously to obtain a uniform suspension. The liquid formulation was converted into free flowing solid one by adsorbing onto calcium carbonate (15 g), talc (2 g) followed by sieving through sieve no. 40. Similarly, a blank S-SNEDDS was prepared using above excipients in same proportion but without using GLP.

For determining drug content, 20 capsules were weighed and mixed. Powder equivalent to 3 mg of GLP was transferred into a 100 mL volumetric flask, and the volume was made up to mark with the mobile phase and was subjected to sonication for about 10 min to solubilize GLP. The resulting solution was filtered through a 0.22 μm nylon filter and injected six times into the HPLC system. Similarly, a blank was prepared in the same way by using blank S-SNEDDS. This process was repeated for three consecutive days. The percentage recovery for each solution ($n = 6$), and mean percentage recovery ($n = 18$) were determined.

3. Results and discussion

3.1. Preliminary investigation

In this study, maximum numbers of factors such as percentage (v/v) of organic phase, buffer pH, flow rate, injection volume, column oven temperature and buffer molarity that affects retention and efficiency in HPLC were selected (Ahuja and Rasmussen, 2007; Snyder et al., 2010). The ranges of individual factors within which a distinct variation of the capacity factor (2–10) can be achieved, were selected based upon the preliminary univariate investigation.

3.2. Analysis of the main effect plot

By visually inspecting the main effect plot of means (Fig. 1a), it shows that retention time was decreased linearly with an increase in percentage (v/v) of acetonitrile (A), flow rate (mL min^{-1}) (C) and buffer molarity (F). No such linear relationships were observed between retention time and other factors such as buffer pH (B), injection volume (D), and column oven temperature (E). Abrupt bending in the main effect lines was observed for all the factors (except percentage (v/v) of acetonitrile) signifying quadratic effect of a concerned factor. From the main effect plot (Fig. 1b), it was found that, tailing factor was increased due to an increase in percentage (v/v) of acetonitrile (A), buffer pH (B), injection volume (μL) (D), and buffer molarity (F). However, no such direct influence

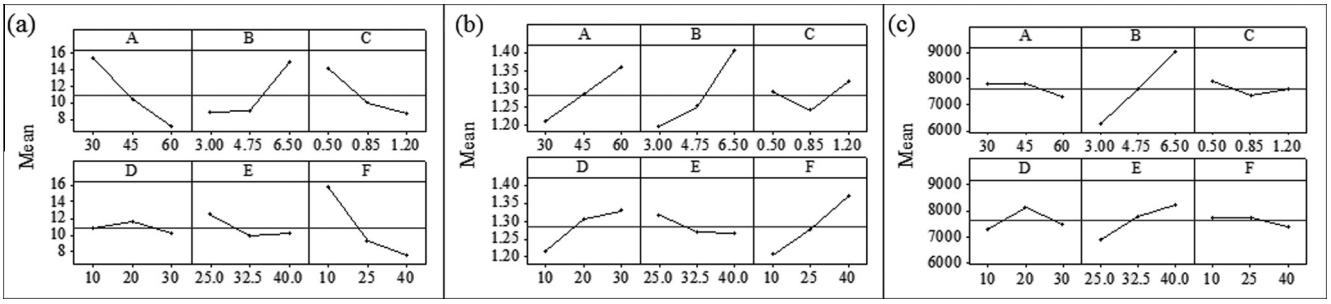

Figure 1 Main effect plots of means for showing the effect of factors (A, B, C, D, E, and F) upon retention time (a), tailing factor (b), and theoretical plate (c). Where A, percentage (v/v) of acetonitrile; B, buffer pH; C, flow rate (mL min^{-1}); D, injection volume (μL); E, column oven temperature (°C) and F, buffer molarity (mM).

upon tailing factor was observed due to flow rate (mL min^{-1}). The sudden bending of the main effect lines in case of factors such as buffer pH (B), flow rate (mL min^{-1}) (C), injection volume (μL) (D) and column oven temperature (°C) (E) justifies their quadratic effect. Similarly, as mentioned in Fig. 1c, theoretical plates were increased by increasing buffer pH (B) as well as the column oven temperature (°C) (E), while rest factors did not a show a linear relationship with theoretical plates.

3.3. Analysis of the S/N ratio and main effect ANOVA

TOA design uses the *S/N* ratio as quality characteristics of three types of *S/N* ratios; the larger is better; the nominal is best; the smaller is better (Sarıkaya and Güllü, 2014). In this study to achieve a better system suitability parameter, "the smaller is a better" *S/N* ratio was selected. Table 2 represents the *S/N* ratio, means, delta values, and ranks of each factor presented at three levels. The *F* ratio obtained from the main effect ANOVA (Table 3) was taken into consideration for calculating the percentage contribution of each factor.

The rankings of factors (based on *S/N* ratio) upon retention time were found to be as percentage (v/v) of acetonitrile (A) > buffer molarity (mM) (F) > buffer pH (B) > flow rate (mL min^{-1}) (C) > column oven temperature (°C) (E) > injection volume (μL) (D). The *F* values and percentage contribution of the individual factors obtained from the main effect ANOVA (Table 3) equally supported the ranking of factors as suggested by *S/N* ratio. However, a slight change in the ranking pattern was observed, as the contribution buffer molarity (mM) (F) was higher than the percentage (v/v) of acetonitrile (A). This might be associated with the errors while calculating the *S/N ratio* in Taguchi design, where interaction between factors is not considered (Montgomery, 2013). Among all the factors, percentage (v/v) of acetonitrile (A), buffer pH (B), flow rate (mL min^{-1}) (C), and buffer molarity (mM) (D) were significantly ($p < 0.05$) affected retention time.

The ranking of factors affecting tailing factor is presented in Table 2, and was found to be in the following order: buffer pH (B) > buffer molarity (mM) (F) > percentage (v/v) of acetonitrile (A) > injection volume (μL) (D) > flow rate (mL min^{-1}) (C) > column oven temperature (°C) (E). This ranking was equally supported from the "*F* value" as obtained in main effect ANOVA (Table 3). All factors (except column oven temperature (°C) (E)) were found to be significantly ($p < 0.05$) affecting tailing factor.

Buffer pH (B) was the alone factor, that had a significant ($p < 0.05$) effect upon theoretical plates, while the rest factors remained non-significant. As per the *S/N* ratio (Table 2) and *F* values (Table 3), the rankings of factors affecting theoretical plates are as buffer pH (B) > column oven temperature (°C) (E) > injection volume (μL) (D) > percentage (v/v) of acetonitrile (A) > buffer molarity (mM) (F) > flow rate (mL min^{-1}) (C).

3.4. Visual interpretation from the contour plots as developed by RSM

Contour plots were analyzed to visualize the effect of the factors on responses. Overlay contour plots describing the effect of significantly contributing factors upon retention time, tailing factor and theoretical plates are shown in Fig. 2a–f. Small blue circles inside contour plots represent actual data points. From contour plots, a region of warm red color presents the highest response; in contrast, a region of deep green color presents the lowest one. It can be observed that a decrease in retention time was associated with an increase in percentage (v/v) acetonitrile (A), Flow rate (mL min^{-1}) (C) and buffer molarity (mM) (F), which is equally supported for the main effect plot (Fig. 1a) as discussed above. Similarly, for tailing factor and theoretical plates, the factors behaved as the same way as mentioned in the main effect plot (Fig. 1b and c). Additionally, Contour plots displayed curvature due to quadratic and/or interaction effect in addition to the linear effects of a factor. This justifies the abrupt bending of response lines in the main effect plot (Fig. 1) as discussed above.

3.5. Analysis of the RSM based models

The observed and predicted values for each response are presented in Table 1. In order to identify the effect (linear, square and interaction) of a factor upon the retention time; the coefficients obtained from regression analysis, were substituted in Eq. (2) to build the model equation for retention time. The model terms having zero coefficients were ignored and the modified equation for retention time is presented in Eq. (3).

Table 2 Response table showing means, signal to noise ratio (S/N), delta value and percentage contribution of each factor.

	A		B		C		D		E		F	
	S/N[a] ratio	Mean	S/N[a] ratio	Mean	S/N[a] ratio	Mean	S/N[a] ratio	Mean	S/N[a] ratio	Mean	S/N[a] ratio	Mean
Retention time												
Level 1	−23.13	15.353	−16.84	8.871	−22.00	14.142	−19.50	10.783	−19.70	12.519	−22.67	15.833
Level 2	−18.74	10.303	−18.25	8.930	−19.18	9.911	−19.15	11.679	−19.13	9.989	−18.38	9.300
Level 3	−15.86	7.020	−22.63	14.876	−16.54	8.623	−19.07	10.214	−18.89	10.169	−16.68	7.543
Delta	7.27	8.333	5.79	6.004	5.47	5.519	0.43	1.464	0.81	2.530	5.98	8.290
Rank	1		3		4		6		5		2	
Tailing factor												
Level 1	−1.568	1.208	−1.507	1.199	−2.155	1.296	−1.634	1.216	−2.337	1.321	−1.546	1.203
Level 2	−2.158	1.289	−1.900	1.251	−1.850	1.243	−2.260	1.306	−2.007	1.267	−2.130	1.284
Level 3	−2.645	1.361	−2.964	1.408	−2.367	1.319	−2.477	1.337	−2.027	1.270	−2.695	1.370
Delta	1.077	0.153	1.457	0.209	0.517	0.076	0.842	0.121	0.330	0.054	1.149	0.167
Rank	3		1		5		4		6		2	
Theoretical plates												
Level 1	−77.58	7770	−75.73	6223	−77.68	7987	−77.01	7264	−76.47	6848	−77.41	7827
Level 2	−77.66	7882	−77.55	7585	−77.19	7374	−77.97	8142	−77.72	7767	−77.71	7739
Level 3	−77.08	7252	−79.03	9097	−77.44	7544	−77.34	7499	−78.13	8290	−77.19	7338
Delta	0.58	630	3.30	2874	0.49	613	0.95	878	1.66	1441	0.52	489
Rank	4		1		6		3		2		5	

A, percentage (v/v) of acetonitrile; B, buffer pH; C, flow rate (mL min^{-1}); D, injection volume (μL); E, temperature of the column oven (°C) and F, buffer molarity (mM).

[a] S/N, signal-to-noise.

Table 3 Result obtained from main effect ANOVA analysis of Taguchi design for responses.

Responses	Effect	*DF*[a]	*F*[b]	*p*[c]	Percentage contribution
Retention time (min)					
	A	2	24.5372	< 0.001*	29.63
	B	2	16.5720	< 0.001*	20.01
	C	2	11.6084	0.001*	14.02
	D	2	0.7590	0.486	0.92
	E	2	2.7747	0.096	3.35
	F	2	26.5719	< 0.001*	32.08
Tailing factor					
	A	2	16.23	< 0.001*	18.96
	B	2	32.60	< 0.001*	38.08
	C	2	4.13	0.039*	4.82
	D	2	10.91	0.001*	12.75
	E	2	2.57	0.112	3.00
	F	2	19.16	< 0.001*	22.38
Theoretical plates					
	A	2	0.5989	0.563	3.66
	B	2	10.9411	0.001*	66.95
	C	2	0.5309	0.599	3.25
	D	2	1.0931	0.362	6.69
	E	2	2.8181	0.094	17.24
	F	2	0.3597	0.704	2.20

[a] *DF*, degree of freedom.

[b] *F*, test for comparing model variance with residual variance.

[c] *p*, probability of seeing the observed *F*-value if the null hypothesis is true.

* Significant at $p < 0.05$.

$$RT = 107.0878 - 1.1365A + 0.0039A^2 - 6.7999B + 0.9611B^2 - 31.185C + 12.0136C^2 + 0.2644D - 0.0118D^2 - 1.6624E + 0.0130E^2 - 0.9736F + 0.0134F^2 + 0.0113AE + 0.0268BE - 0.0025CE + 0.0055DE + 0.0055AF - 0.0594BF + 0.1184CF \quad (3)$$

where *RT*, retention time (min); *A*, percentage (v/v) of acetonitrile; *B*, buffer pH; *C*, flow rate (mL min^{-1}); *D*, injection volume (μL); *E*, column oven temperature (°C) and *F*, buffer molarity (mM). The relationship between observed and predicted retention time was found to be linear with a good correlation coefficient (adjusted $R^2 = 0.9152$), where a value of the adjusted R^2 greater than equal to 0.8 (adjusted $R^2 \geqslant 0.8$) can be considered as acceptable for chemical samples (Lundstedt et al., 1998). The average difference between the predicted and experimental retention time was approximately 0.87 min and the largest difference was 1.66 min. The model *F*-value (15.76) along with $p < 0.001$ for the whole model implied that the model is significant.

A mathematical model was derived for the tailing factor as below in Eq. (4) after ignoring the model terms having a zero coefficient.

$$TF = 1.533061 + 0.003679A - 0.00002A^2 - 0.082472B + 0.017052B^2 - 0.800113C + 0.521542C^2 + 0.008806D - 0.000294D^2 - 0.028522E + 0.000257E^2 + 0.011093F + 0.00001F^2 + 0.000952BE + 0.000317CE + 0.000278DE + 0.000128AF - 0.002032BF - 0.00254CF \quad (4)$$

where *TF*, tailing factor; *A*, percentage (v/v) of acetonitrile; *B*, buffer pH; *C*, flow rate (mL min^{-1}); *D*, injection volume (μL);

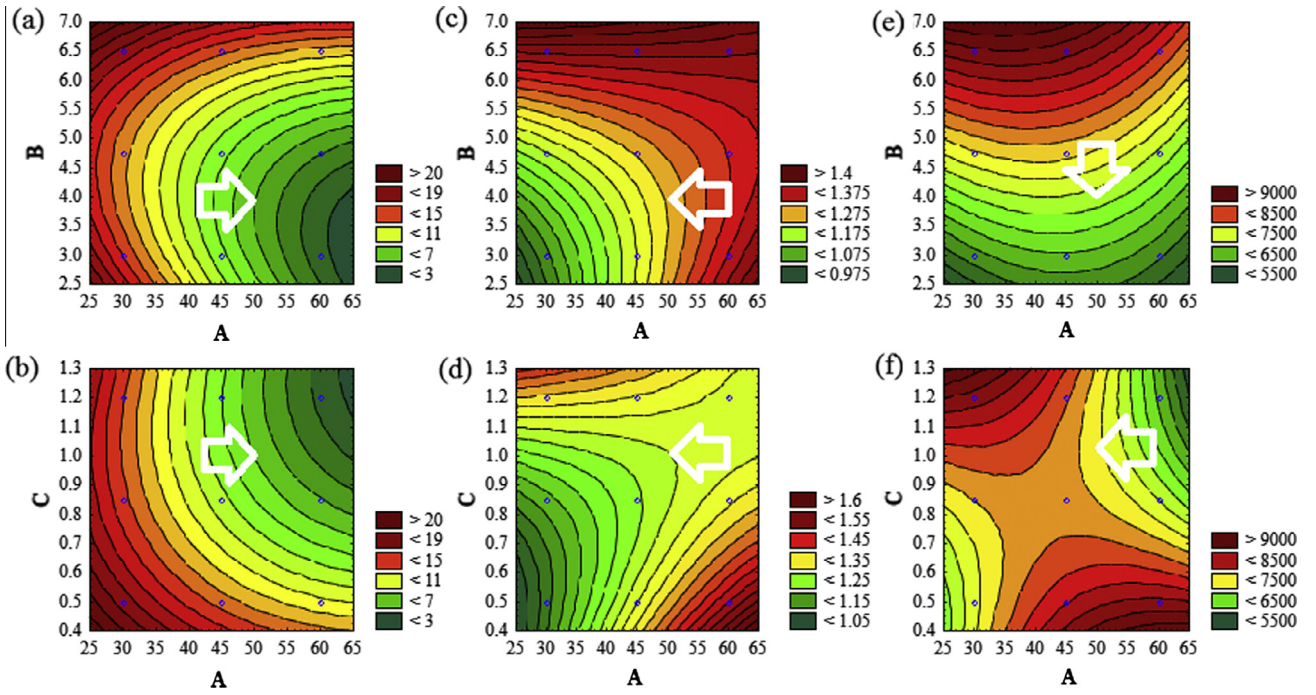

Figure 2 Contour plots for retention time (a, b), for tailing factor (c, d) and for theoretical plates (e, f). Where; A, percentage (v/v) of acetonitrile; B, buffer pH and C, flow rate (mL min^{-1}). Small blue circles represent actual data points. White arrow marks represent optimized region.

E, column oven temperature (°C) and *F*, buffer molarity (mM). The model *F*-value of 13.12 with $p < 0.001$ implied that the model was significant. The relationship between observed and predicted tailing factor was found to be linear, having a good correlation coefficient (adjusted $R^2 = 0.8985$). The average and largest differences between predicted and experimental tailing factor were found to be 0.019 and 0.06 respectively.

Similarly, the relation between theoretical plates and different factors was presented as the model equation below (Eq. (5)).

$$\begin{aligned} TP = {} & -12430.3 + 220.2A - 1.6A^2 + 1260.1B + 24.5B^2 \\ & - 1833.6C + 3195.9C^2 + 517.1D - 7.6D^2 + 197.2E \\ & + 2.3E^2 + 237.2F - 0.8F^2 - 0.5AE + 0.2BE \\ & - 170.3CE - 6.2DE - 2.9AF - 27.1BF + 52.1CF \end{aligned} \quad (5)$$

where *TP*, theoretical plates; *A*, percentage (v/v) of acetonitrile; *B*, buffer pH; *C*, flow rate (mL min^{-1}); *D*, injection volume (μL); *E*, column oven temperature (°C) and *F*, buffer molarity (mM). The Model "*F*-value" of 9.99 along with $p < 0.001$ implied the model is significant. The relationship between observed and predicted theoretical plates was found to be linear with an acceptable correlation coefficient (adjusted $R^2 = 0.8679$). The average difference between predicted and observed theoretical plates was approximately 264, with the largest difference of 735.

3.6. Adequacies of the RSM based models

From the residual versus predicted plot (Fig. 3a–c), it can be observed that the residuals for each response exhibited a homogeneous pattern. Moreover, residuals were found to be structure-less and independent with an almost equal scatter above and below the zero-line of the residual plot. This implies that the proposed models are adequate and the variance of the experimental measurements is constant at all values of responses. Hence, there is no reason to suspect any violation of the independence or constant variance assumption (Montgomery, 2013). Therefore, these models can be successfully used for the prediction of responses.

3.7. Derringer's desirability for responses

Derringer's desirability function uses a dimensionless desirability value (*d*). The scale of *d* varies between 0 and 1. If $d = 0$, then the response is undesirable to $d = 1$, where the response is fully desirable. Hence, a value of 1 or closer to 1 is required for getting a response of perfect target value (Derringer and Suich, 1980). The individual desirability values can be summed up to get a single value called global desirability (d_G) and can be represented as Eq. (6).

$$d_G = [d_1^{p1} x d_2^{p2} x \ldots x . d_n^{pn}]^{1/n} \quad (6)$$

where $d_1 \ldots d_n$ is the individual desirability for $1 \ldots n$ number of responses; *p* is the weight of the responses and was set equal to 1. The goal used for retention time and tailing factor was minimized, whereas the goal was maximized for theoretical plates.

3.8. Optimization of the chromatographic method

Analyzing the obtained three-dimensional graphs, *S*/*N* ratio, percentage contribution of each factor and desirability,

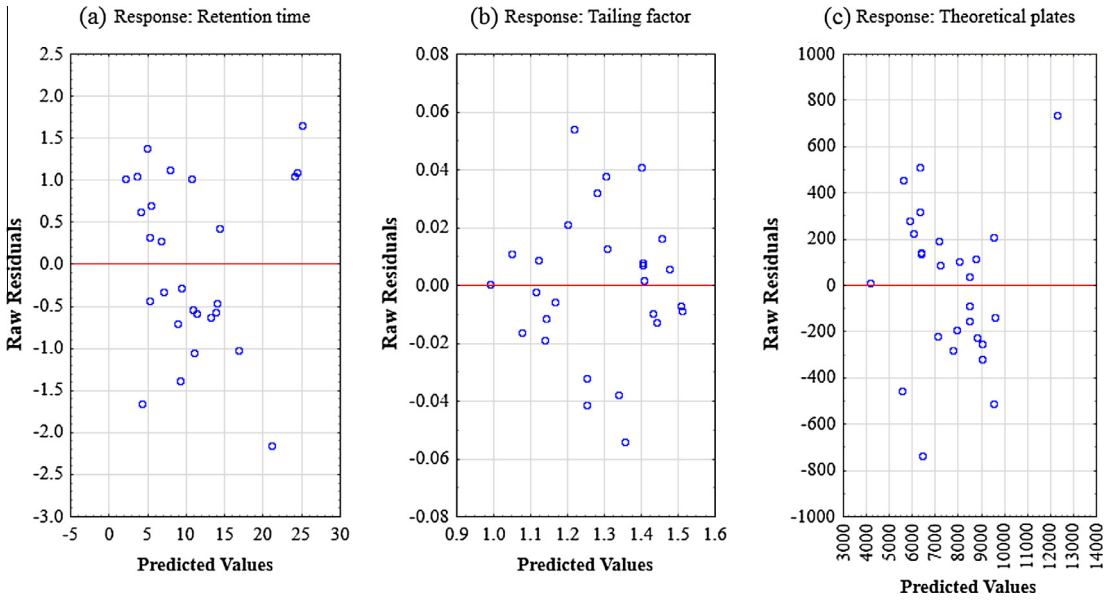

Figure 3 Predicted versus residual plot for retention time (a), tailing factor (b), and theoretical plates (c).

optimal chromatographic conditions were defined to get a chromatogram with lower tailing factor, higher theoretical plates and a suitable capacity factor along with a reasonable resolution to separate GLP from its major degradation products formed under various stress conditions. White color arrow mark inside the contour plots (Fig. 2a–f) represents the optimized region.

The global desirability was found to be close to 1 for each response (RT = 0.982; TF = 0.982; TP = 0.951) at the following optimum conditions. Optimal conditions for the separation of GLP were achieved at a temperature of 35 ± 2 °C using acetonitrile – potassium dihydrogen phosphate (pH 4.0; 30 mM) (50:50, v/v). The flow rate was kept at 1.0 mL min^{-1} while the injection volume selected as 20 µL. The detection wavelength selected was 229 nm.

These chromatographic conditions delivered chromatogram having a reasonable capacity factor (4.37) with better plate count (7020) and lower tailing factor (1.25). The resolutions between GLP, and its nearest degradants peak were found to be greater than equal to 5.66, which was higher than the required level ($R_s \geqslant 1.80$) (Fig. 4). This in turn satisfied the predetermined optimization goal criteria. To confirm these obtained results, six replicates injections of GLP (20 µg mL^{-1}) were analyzed as a confirmatory experiment during system suitability testing.

3.9. Method validation

3.9.1. Linearity, precision, accuracy, LOD and LOQ

GLP was found to be linear over the range 0.05–100 µg mL^{-1} with a high correlation coefficient (0.999). The regression equation for the calibration curve was found to be as below in Eq. (7).

$$y = 32308x - 1227 \quad (7)$$

where y is the peak area (µV s) and x, the concentration of GLP (µg mL^{-1}). The relative standard deviations for intra-day and inter-day precisions were found to be less than 2%, indicating that the method was precise. In addition, accuracy was found to be high, having a mean percentage recovery of 100.22. LOD and LOQ were found to be 0.02 and 0.05 µg mL^{-1} respectively.

3.9.2. Specificity

The specificity of the HPLC method is illustrated in Figs. 4 and 5, where a complete separation of GLP in the presence of its degradation products and excipients of S-SNEDDS (blank S-SNEDDS) was noticed. The average retention time for GLP was found to be 5.91 min. The peaks obtained were sharp having clear baseline separation.

3.9.3. Robustness of the method

The results for robustness were remained unaffected by small variations of the chromatographic parameters. The result from the two columns indicated that there was no significant difference between the results from the two columns. Nonsignificant differences in retention time, tailing factor and theoretical plates were observed.

3.9.4. System suitability

In the final step, the optimization was verified by six confirmatory experiments and can be regarded as the system suitability testing. The results for system suitability were found to be within the acceptable limits.

3.10. Stability-indicating property

An analytical method is stability indicating if it can separate all the process-related impurities and degradation products from the parent peak. No degradation peaks were eluted from the degradation mixture after the parent peak at 5.91–15 min; hence, the run time was selected as 10 min for individual degradation samples. The overlay chromatogram obtained from all the degradation conditions is presented in Fig. 4. GLP was found to be highly degraded in acidic media, where 91% of GLP were degraded by 48 h. GLP also found

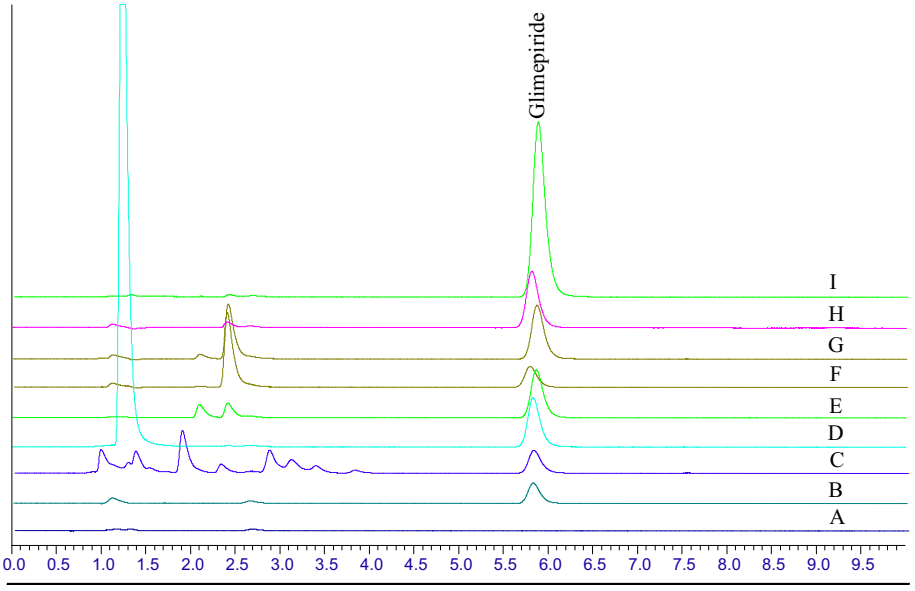

Figure 4 Overlay chromatogram for A, blank; B, acid degradation; C, base degradation; D, oxidative degradation; E, hydrolytic degradation; F, dry heat degradation; G, moist heat degradation; H, photolytic degradation and I, standard GLP (20 μg mL^{-1}).

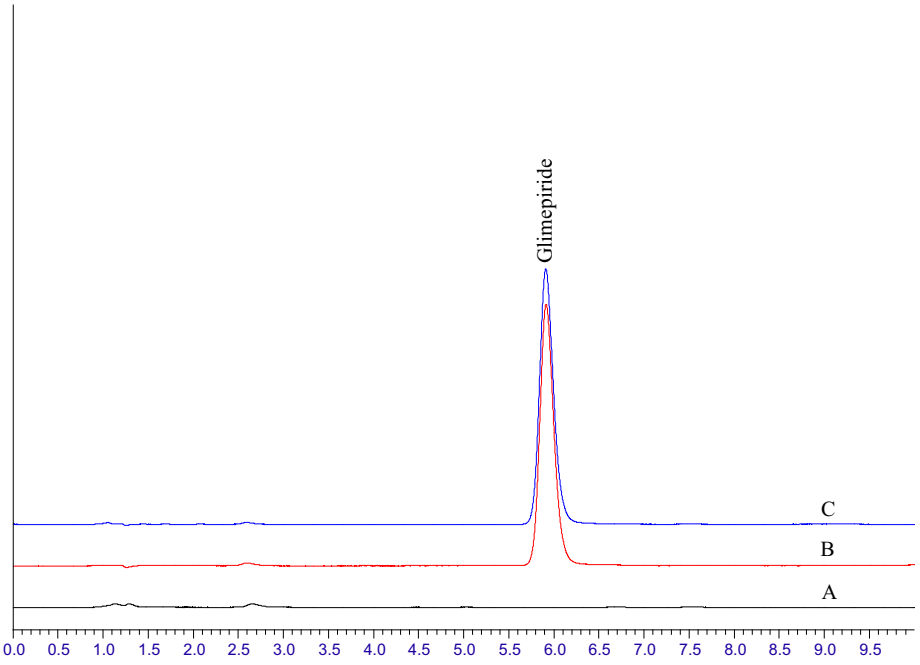

Figure 5 Overlay chromatogram of A, S-SNEDDS blank; B, standard GLP (30 μg mL^{-1}) and C, S-SNEDDS of GLP.

to be highly labile in basic media and was degraded by 90% in 48 h. Oxidized stressed condition showed a major degradation peak at 1.21 min, and around 78% of GLP was found to be degraded by 6 h. Hydrolytic degradation formed two distinct degradation peaks (at 2.10 and 2.40 min), and 78% of GLP was found to be degraded at the end of fifth days. Dry heat and moist heat induced degradation gave rise to a common degradation peak at 2.40 min. GLP was degraded by 90% and 75% during dry heat and moist heat stressed conditions respectively. Photolytic degradation eluted one degradation peak (at 2.40 min) and degraded GLP by 75%. A common degradation peak (at 2.40 min) was observed in case of hydrolytic, dry heat, moist heat and photolytic condition, while a degradation peak (at 2.10 min) was found to be common for both hydrolytic and moist heat stressed conditions.

These results indicate that GLP is susceptible to acid-base hydrolysis, oxidative, thermal and photo degradation. Adequate resolutions ($R_s \geqslant 5.66$) between GLP and its nearest degradation peaks were obtained under the different stressed conditions. In all cases above, no degradation peaks were found to interfere or co-eluted with GLP suggesting the

method enabled specific analysis of GLP in the presence of its degradation products.

3.11. Analysis of GLP S-SNEDDS

From Fig. 5, it was observed that, no peaks from the excipient (S-SNEDDS blank) were co-eluted at the GLP retention time. The mean recovery of GLP from S-SNEDDS was found to be 100.29% indicating the non-interference from excipients. Hence, the method is suitable for the quantification of GLP in the S-SNEDDS formulation.

4. Conclusion

This study demonstrated the worth of Taguchi orthogonal array design combined with a response surface methodological approach for the development of a robust stability indicating HPLC method for the GLP. This approach exposed the two-way interactions between factors, which were impossible to detect with the Taguchi design alone. The critical factors that are significantly ($p < 0.05$) affecting the studied responses were identified and controlled to achieve the predetermined method goal. The best method having improved system suitability parameters was employed in the routine assay of GLP from an S-SNEDDS formulation. Lastly, the presented data in the future will help analysts to diagnose any problems along with corrective action, which may come across during the life cycle of the stated stability indicating method, if applied for other purposes involving quantitative estimation of glimepiride provided specificity is justified for the intended purpose.

Acknowledgements

Authors are thankful to Abitec Corp., Janesville, USA; Gattefosse Corp., San-Priest, France; BASF SE, Ludwigshafen, Germany, and Sasol olefins and surfactants, GmbH, Germany for providing excipients used during this study.

Appendix A. Supplementary material

Supplementary data associated with this article can be found, in the online version, at http://dx.doi.org/10.1016/j.jsps.2015.03.004.

References

Aburuz, S., Millership, J., McElnay, J., 2005. The development and validation of liquid chromatography method for the simultaneous determination of metformin and glipizide, gliclazide, glibenclamide or glimperide in plasma. J. Chromatogr. B Anal. Technol. Biomed. Life Sci. 817, 277–286.

Aggarwal, A., Singh, H., Kumar, P., Singh, M., 2008. Optimizing power consumption for CNC turned parts using response surface methodology and Taguchi's technique—a comparative analysis. J. Mater. Process. Technol. 200, 373–384.

Ahuja, S., Rasmussen, H., 2007. HPLC Method Development for Pharmaceuticals, first ed. Elsevier, Amsterdam, London.

Awotwe-Otoo, D., Agarabi, C., Faustino, P.J., Habib, M.J., Lee, S., Khan, M.A., Shah, R.B., 2012. Application of quality by design elements for the development and optimization of an analytical method for protamine sulfate. J. Pharm. Biomed. Anal. 62, 61–67.

Bandyopadhyay, S., Katare, O.P., Singh, B., 2012. Optimized self nano-emulsifying systems of ezetimibe with enhanced bioavailability potential using long chain and medium chain triglycerides. Colloids Surf. B Biointerfaces 100, 50–61.

Bansal, G., Singh, M., Jindal, K.C., Singh, S., 2008. LC-UV-PDA and LC-MS studies to characterize degradation products of glimepiride. J. Pharm. Biomed. Anal. 48, 788–795.

Bezerra, M.A., Santelli, R.E., Oliveira, E.P., Villar, L.S., Escaleira, L.A., 2008. Response surface methodology (RSM) as a tool for optimization in analytical chemistry. Talanta 76, 965–977.

Bonfilio, R., Peres, C., Salgado, H.R., De Araújo, M.B., Tarley, C.R., 2013. Multivariate development and validation of a stability-indicating HPLC method for the determination of glimepiride in tablets. J. AOAC Int. 96, 960–967.

Brittain, H.G., 2009. Profiles of Drug Substances, Excipients and Related Methodology, first ed. Academic Press, London.

Chakradhar, L., Kallem, R., Karthik, A., Sundari, B.T., Ramesh, S., Mullangi, R., Srinivas, N.R., 2008. A rapid and highly sensitive method for the determination of glimepiride in human plasma by liquid chromatography-electrospray ionization tandem mass spectrometry: application to a pre-clinical pharmacokinetic study. Biomed. Chromatogr. 22, 58–63.

Chang, J.S., Huang, Y.B., Hou, S.S., Wang, R.J., Wu, P.C., Tsai, Y.H., 2007. Formulation optimization of meloxicam sodium gel using response surface methodology. Int. J. Pharm. 338, 48–54.

Derringer, G., Suich, R., 1980. Simultaneous optimization of several response variables. J. Qual. Technol. 12, 214–220.

El Deeb, S., Schepers, U., Wätzig, H., 2006. Fast HPLC method for the determination of glimepiride, glibenclamide, and related substances using monolithic column and flow program. J. Sep. Sci. 29, 1571–1577.

El-Enany, N.M., Abdelal, A.A., Belal, F.F., Itoh, Y.I., Nakamura, M.N., 2012. Development and validation of a repharsed phase-HPLC method for simultaneous determination of rosiglitazone and glimepiride in combined dosage forms and human plasma. Chem. Cent. J. 6 (9), 1–10.

Gao, P., Morozowich, W., 2006. Development of supersaturatable self-emulsifying drug delivery system formulations for improving the oral absorption of poorly soluble drugs. Expert Opin. Drug Deliv. 3, 97–110.

Gao, P., Akrami, A., Alvarez, F., Hu, J., Li, L., Ma, C., Surapaneni, S., 2009. Characterization and optimization of AMG 517 supersaturatable self-emulsifying drug delivery system (S-SEDDS) for improved oral absorption. J. Pharm. Sci. 98, 516–528.

Hibbert, D.B., 2012. Experimental design in chromatography: a tutorial review. J. Chromatogr. B Anal. Technol. Biomed. Life Sci. 910, 2–13.

International conference on harmonisation of technical requirements for registration of pharmaceuticals for human use, Draft Step 4. Validation of analytical text procedures: Text and methodology Q2 (R1), 2005.

Jain, D., Jain, S., Jain, D., Amin, M., 2008. Simultaneous estimation of metformin hydrochloride, pioglitazone hydrochloride, and glimepiride by RP-HPLC in tablet formulation. J. Chromatogr. Sci. 46, 501–504.

Karthik, A., Subramanian, G., Mallikarjuna Rao, C., Bhat, K., Ranjithkumar, A., Musmade, P., Surulivelrajan, M., Karthikeyan, K., Udupa, N., 2008. Simultaneous determination of pioglitazone and glimepiride in bulk drug and pharmaceutical dosage form by RP-HPLC method. Pak. J. Pharm. Sci. 21, 421–425.

Khan, M.A., Sinha, S., Vartak, S., Bhartiya, A., Kumar, S., 2005. LC determination of glimepiride and its related impurities. J. Pharm. Biomed. Anal. 39, 928–943.

Kovaríková, P., Klimes, J., Dohnal, J., Tisovská, L., 2004. HPLC study of glimepiride under hydrolytic stress conditions. J. Pharm. Biomed. Anal. 36, 205–209.

Kwak, J.-S., 2005. Application of Taguchi and response surface methodologies for geometric error in surface grinding process. Int. J. Mach. Tools Manuf 45, 327–334.

Lakshmi, K.S., Rajesh, T., 2011. Development and validation of RP-HPLC method for simultaneous determination of glipizide, rosiglitazone, pioglitazone, glibenclamide and glimepiride in pharmaceutical dosage forms and human plasma. J. Iran. Chem. Soc. 8, 31–37.

Lundstedt, T., Seifert, E., Abramo, L., Thelin, B., Nystrom, A., Pettersen, J., Bergman, R., 1998. Experimental design and optimization. Chemomet. Intell. Lab. Syst. 42, 3–40.

Maier, V., Znaleziona, J., Jirovsky, D., Skopalova, J., Petr, J., Sevcik, J., 2009. Determination of antihyperglycemic drugs in nanomolar concentration levels by micellar electrokinetic chromatography with non-ionic surfactant. J. Chromatogr. A 1216, 4492–4498.

Montgomery, D.C., 2013. Design and Analysis of Experiments, eighth ed. John Wiley & Sons Inc, Hoboken, NJ.

Musmade, P.B., Talole, K.B., Deshpande, P.B., Karthik, A., Pathak, S.M., Pandey, S., Udupa, N., 2011. Novel liquid chromatographic method for simultaneous estimation of pioglitazone and glimepiride in rat plasma by solid phase extraction: application to preclinical pharmacokinetic studies. Arzneimittelforschung 61, 23–31.

Pandit, V., Pai, R.S., Devi, K., Singh, G., Narayana, S., Suresh, S., 2012. Development and validation of the liquid chromatographic method for simultaneous estimation of metformin, pioglitazone, and glimepiride in pharmaceutical dosage forms. Pharm. Methods 3, 9–13.

Pistos, C., Koutsopoulou, M., Panderi, I., 2005. Improved liquid chromatographic tandem mass spectrometric determination and pharmacokinetic study of glimepiride in human plasma. Biomed. Chromatogr. 19, 394–401.

Polagani, S.R., Pilli, N.R., Gajula, R., Gandu, V., 2013. Simultaneous determination of atorvastatin, metformin and glimepiride in human plasma by LC–MS/MS and its application to a human pharmacokinetic study. J. Pharm. Anal. 3, 9–19.

Rafamantanana, M.H., Debrus, B., Raoelison, G.E., Rozet, E., Lebrun, P., Uverg-Ratsimamanga, S., Hubert, P., Quetin-Leclercq, J., 2012. Application of design of experiments and design space methodology for the HPLC-UV separation optimization of aporphine alkaloids from leaves of Spirospermum penduliflorum Thouars. J. Pharm. Biomed. Anal. 62, 23–32.

Salem, I.I., Idrees, J., Al Tamimi, J.I., 2004. Determination of glimepiride in human plasma by liquid chromatography-electrospray ionization tandem mass spectrometry. J. Chromatogr. B Anal. Technol. Biomed. Life Sci. 799, 103–109.

Samala, S., 2011. Determination of Glimepiride in Rat Serum by RP-HPLC Method. Am. J. Anal. Chem. 02, 152–157.

Sarıkaya, M., Güllü, A., 2014. Taguchi design and response surface methodology based analysis of machining parameters in CNC turning under MQL. J. Clean. Prod. 65, 604–616.

Shaligram, N.S., Singh, S.K., Singhal, R.S., Szakacs, G., Pandey, A., 2008. Compactin production in solid-state fermentation using orthogonal array method by *P. brevicompactum*. Biochem. Eng. J. 41, 295–300.

Shaodong, J., Lee, W.J., Ee, J.W., Park, J.H., Kwon, S.W., Lee, J., 2010. Comparison of ultraviolet detection, evaporative light scattering detection and charged aerosol detection methods for liquid-chromatographic determination of anti-diabetic drugs. J. Pharm. Biomed. Anal. 51, 973–978.

Snyder, L.R., Kirkland, J.J., Dolan, J.W., 2010. Introduction to Modern Liquid Chromatography, third ed. Wiley, Hoboken, NJ.

Sweetman, S.C., 2009. Martindale: The Complete Drug Reference, thirty sixth ed. Pharmaceutical Press, London, Chicago.

Taguchi, G., 1987. System of experimental design: engineering methods to optimize quality and minimize costs. UNIPUB/Kraus International Publications, American Supplier Institute, White Plains, N.Y. Dearborn, Mich.

Tripathi, A.S., Dewani, A.P., Shelke, P.G., Bakal, R.L., Chandewar, A.V., Mazumder, P.M., 2013. Development and validation of RP-HPLC method for simultaneous estimation of glimepiride and sildenafil citrate in rat plasma-application to pharmacokinetic studies. Drug. Res. (Stuttg) 63, 510–514.

Wei, Y., Ye, X., Shang, X., Peng, X., Bao, Q., Liu, M., Guo, M., Li, F., 2012. Enhanced oral bioavailability of silybin by a supersaturatable self-emulsifying drug delivery system (S-SEDDS). Colloids Surf., A 396, 22–28.

Yao, J., Shi, Y.Q., Li, Z.R., Jin, S.H., 2007. Development of a RP-HPLC method for screening potentially counterfeit anti-diabetic drugs. J. Chromatogr. B Anal. Technol. Biomed. Life Sci. 853, 254–259.